Journal of the National Cancer Center 4 (2024) 369–381

Contents lists available at ScienceDirect

Journal of the National Cancer Center

journal homepage: www.elsevier.com/locate/jncc

Full Length Article

S100A8 promotes tumor progression by inducing phenotypic polarization of microglia through the TLR4/IL-10 signaling pathway in glioma

Yuechao Yang [1,2,†], Huanhuan Cui [1,2,†], Deheng Li [1,2], Lei Chen [1,2], Yi Liu [3], Changshuai Zhou [1,2], Liangdong Li [1,2], Mingtao Feng [1,2], Xin Chen [1,2,*], Yiqun Cao [1,2,*], Yang Gao [1,2,*]

[1] Department of Neurosurgery, Fudan University Shanghai Cancer Center, Shanghai, China
[2] Department of Oncology, Shanghai Medical College, Fudan University, Shanghai, China
[3] School of Basic Medical Sciences, Fudan University, Shanghai, China

ARTICLE INFO

Keywords:
S100A8
Glioma
Microglia
TLR4
IL-10

ABSTRACT

Background: S100A8 is a member of the S100 protein family and plays a pivotal role in regulating inflammation and tumor progression. This study aimed to comprehensively assess the expression patterns and functional roles of S100A8 in glioma progression.

Methods: Glioma tissues were collected from 98 patients who underwent surgical treatment at Fudan University Shanghai Cancer Center. S100A8 expression in glioma tissues was analyzed using immunohistochemistry (IHC) to establish its correlation with clinicopathological features in patients. The expression and prognostic effect of S100A8 in glioma were analyzed using TCGA and CGGA public databases. Then, we investigated the role of S100A8 in glioma through a series of *in vivo* and *in vitro* experiments including Transwell, wound healing, CCK8, and intracranial tumor models. Subsequently, bioinformatics analysis, single-cell sequencing and coimmunoprecipitation (Co-IP) were used to explore the underlying mechanism.

Results: S100A8 was upregulated in gliomas compared to paracancerous tissues, and this phenotype was significantly correlated with poor prognosis. Subgroup analysis showed that S100A8 expression was higher in the high-grade glioma (HGG) group than that in the low-grade glioma (LGG) group. S100A8 overexpression in glioma cell lines promoted cell proliferation, migration and invasion, while silencing S100A8 reversed these effects. *In vivo* experiments showed that S100A8 knockdown can significantly reduce the tumor burden of glioma cells. Notably, S100A8 was observed to stimulate microglial M2 polarization by interacting with TLR4, which subsequently induced NF-κB signaling and IL-10 secretion within the tumor microenvironment.

Conclusions: S100A8 promotes tumor progression by inducing phenotypic polarization of microglia through the TLR4/IL-10 signaling pathway in glioma. It might represent a therapeutic target for further basic research or clinical management of glioma.

1. Introduction

Glioma represents a rare yet highly malignant tumor that poses substantial treatment challenges. As the predominant primary intracranial malignancy, it constitutes approximately 40–50% of intracranial tumors, with an incidence of 3–8 cases per 100,000 individuals. Based on the World Health Organization (WHO) classification, gliomas are categorized into grades I–IV; a higher grade is correlated with increased malignancy and poorer prognosis.[1] Glioblastoma multiforme (GBM) represents grade IV glioma, which has the highest degree of intracranial malignancy. Characterized by extensive invasiveness and a propensity for relapse, GBM continues to pose clinical challenges even following surgical resection, postoperative radiotherapy, chemotherapy and other standardized comprehensive treatments.[2,3] Despite advancements in GBM treatment, patient survival rates have not significantly improved. The median survival time remains short at 14.6 months, with the majority of patients experiencing relapse within six months. Notably, the 5-year survival rate remains below 5%.[4–6]

S100 calcium binding protein A8 (S100A8) is a calcium and zinc binding protein known for its pivotal role in regulating inflammatory processes and immune responses. Notably, it induces neutrophil chemotaxis and adhesion. Functionally, S100A8 primarily operates as a dimer,

* Corresponding authors at: Department of Neurosurgery, Fudan University Shanghai Cancer Center, Shanghai, China.
E-mail addresses: ghost_dinosaur@163.com (X. Chen), yiqun_fduscc@163.com (Y. Cao), dryanggao@126.com (Y. Gao).
† These authors have contributed equally to this work.

https://doi.org/10.1016/j.jncc.2024.07.001
Received 23 January 2024; Received in revised form 11 July 2024; Accepted 14 July 2024

partnering with S100A9 to exert its effects. S100A8/A9 is a member of the S100 protein family that binds to Ca^{2+} and has gained significant interest as a crucial protein that controls inflammatory reactions after its release (as extracellular S100A8/A9) from neutrophils and monocytes.[7,8] Furthermore, S100A8 exhibits a diverse range of intracellular and extracellular functions. Intracellularly, it facilitates arachidonic acid transport, impacts white blood cell metabolism, and regulates the cytoskeleton during phagocyte movement. Outside cells, it promotes inflammation, combats bacteria, mitigates oxidation, and triggers apoptosis. Notably, its proinflammatory actions encompass leukocyte attraction, cytokine and chemokine stimulation, and control of myeloid cell adhesion and motility. While S100A8 is abundant in immune cells such as neutrophils, it is also highly expressed in tumor cells. Recent investigations underscore its significant role in tumorigenesis, with reported involvement in cervical squamous cell carcinoma, colon cancer, renal clear cell carcinoma, and pancreatic cancer. Enhanced S100A8 expression has been observed in breast cancer and various other tumors, and its high expression in glioma has been linked to unfavorable patient prognosis. Thus, S100A8 serves as a molecular marker of adverse prognosis.[9–12]

The distinct immune microenvironments of cancer cells have garnered extensive recognition, as various immune cells within these environments play roles in supporting processes such as cell proliferation, distant tumor metastasis, and immune evasion. In contrast to extracranial tumors, intracranial tumors lack immune cells like T and B cells. Nevertheless, they harbor a substantial number of tumor-associated macrophages (TAMs), predominantly represented by brain microglia.[13,14] Glioblastoma-associated macrophages/microglia constitute a high proportion of immune cells (up to 50% of the total glioblastoma cell population). Recent investigations underscore the symbiotic interplay between GBM cells and TAMs as pivotal for tumor growth and progression.[15–17] Notably, GBM exhibits unique metabolic traits that enable communication with the surrounding tumor microenvironment. Through this metabolic mode, GBM stimulates the secretion of pertinent chemokines and cytokines that influence the chemokine dynamics and functions of neighboring immune cells. This process contributes to tumor initiation, progression, migration, invasion, recurrence, and drug resistance.

Overall, this study aimed to explore the clinical relevance of S100A8 and elucidate its regulatory role in glioma development, particularly its involvement in driving microglial polarization within the tumor microenvironment.

2. Materials and methods

2.1. Clinical characteristics

Glioma tissues were collected from 98 patients who underwent surgical treatment at Fudan University Shanghai Cancer Center (FUSCC, shanghai, China) between April 2020 and January 2023 including 11 samples of para-carcinoma tissue, 7 samples of grade I glioma, 32 samples of grade II glioma, 23 samples of grade III glioma and 36 samples of grade IV glioma. Tissue microarrays (TMA) was constructed as previously described.[18] The expression of S100A8 in glioma was evaluated by immunohistochemistry (IHC). Patients' information including sex, age and tumor grade was summarized in Table 1. The correlation between S100A8 and clinicopathological data (IDH1, 1p19q) and prognosis were also analyzed utilizing datasets from The Cancer Genome Atlas (TCGA) and Chinese Glioma Genome Atlas (CGGA) (Supplementary Fig. 1).

2.2. Immunohistochemical staining assay

IHC was performed according to previous protocols using S100A8 antibodies (Cat. #ab288715; Abcam, Cambridge, MA, USA).[19] Pictures were taken under a microscope (OLYMPUS) and analyzed with ImageJ. Two pathologists evaluated the expression of S100A8 by using the IHC scoring method.[20] For staining intensity quantification, we used a scoring system: 0 (negative), 1 (weak), 2 (medium), and 3 (strong). To evaluate staining extent, scores were assigned based on the percentage of positively stained area relative to the entire cancerous region: 0 (<5%), 1 (5–25%), 2 (26–50%), 3 (51–75%), and 4 (>75%). The immunoreactivity score was determined by multiplying the intensity and percentage scores. According to the immunohistochemical score of S100A8, the samples were divided into two groups: the top 50% of the score was the high expression group, and the bottom 50% was the low expression group, to analyze its correlation with the clinicopathological factors of glioma.

2.3. Cell lines and culture

The human glioma cell lines (U87 and U251) and the HMC3 human microglia cell line were purchased from the Chinese Academy of Sciences (Shanghai, China). The cells were grown in DMEM with the addition of 10% fetal bovine serum and 1% penicillin/streptomycin (Gibco, Invitrogen, USA). Incubation of all cells was carried out at 37°C in the presence of 5% carbon dioxide.

2.4. Transient cell transfection

Glioma cells were transfected with siRNAs using Lipofectamine 3000 reagent (Invitrogen, California, USA) according to the manufacturer's instructions. The siRNAs against S100A8 (siS100A8) and the control were obtained from Gemma Gene (Shanghai, China). Cells were collected 48 hours after transfection. The siRNA sequences of S100A8 are listed in Supplementary Table 1.

Table 1
Association of S100A8 expression with clinicopathological parameters.

Characteristic	S100A8 high expression (n = 54)	S100A8 low expression (n = 55)	P value
Grade, n (%)			< 0.001
–	1 (0.9)	10 (9.2)	
1	0 (0.0)	7 (6.4)	
2	7 (6.4)	25 (22.9)	
3	14 (12.8)	9 (8.3)	
4	32 (29.4)	4 (3.7)	
Sex, n (%)			0.904
Female	20 (18.3)	22 (20.2)	
Male	34 (31.2)	33 (30.3)	
Tissue types, n (%)			0.012
Normal	1 (0.9)	10 (9.2)	
Tumor	53 (48.6)	45 (41.3)	
Age, mean ± SD, years	46.24 ± 8.6	41.29 ± 10.65	0.009

2.5. Lentivirus infection

To create cell lines with stable knockdown and overexpression of S100A8, we stably infected cells with lentiviral particles containing pLKO.1-LUC-puro-S100A8 shRNA (Tsingke Biotech, Beijing, China) and GV492-gcGFP-puro-S100A8 (Genechem, Shanghai, China). To summarize, HEK293T cells were simultaneously transfected with pLKO.1 or GV492 along with the packaging plasmids (psPAX2 and pMD2G). Following 72 hours of transfection, the lentiviral particles were collected and filtered using a 0.45-μm membrane. Glioma cells were exposed to lentiviral particles and polybrene. After being screened with puromycin for a period of 3–4 weeks, the stable cell lines were utilized in subsequent experiments once their S100A8 expression was confirmed through RT–qPCR and western blotting.

2.6. Quantitative reverse transcriptase-polymerase chain reaction (RT–qPCR)

PrimeScript RT Master Mix (Takara, Osaka, Japan) was utilized for reverse transcription following the extraction of total RNA from the cells using TRIzol (Invitrogen, California, USA). Real-time qPCR was performed using SYBR Premix. The evaluation of RNA extraction, reverse transcription, and real-time qPCR was conducted following the methods described earlier.[19] The primers are listed in Supplementary Table 1. Next, the mRNA level was standardized to the GAPDH mRNA level, and the relative expression of each mRNA was determined using the 2-ΔΔCt technique.

2.7. Western blotting and co-immunoprecipitation (Co-IP) assays

Total protein was extracted from cell lines, and western blotting was performed according to a previously described method.[21] The membranes were incubated in sealing fluid for 10 min at room temperature and then with primary antibodies against S100A8 (Cat. #ab288715; Abcam; 1:1000), CD163 (Cat. #DF8235; Affinity; 1:1000), ARG1 (Cat. #DF6657; Affinity; 1:1000), TLR4 (Cat. #66350-1-Ig; Proteintech; 1:5000), IL-10 (Cat. #60269-1-Ig; Proteintech; 1:5000), p65 (Cat. #80979-7-RR; Proteintech; 1:5000), p-p65 (Cat. #3033S; Cell Signaling Technology; 1:1000), JAK1 (Cat. #AF5012; Affinity; 1:1000), STAT3 (Cat. #AF6294; Affinity; 1:1000), and β-actin (Cat. #81115-1-RR; Proteintech; 1:5000) at 4°C overnight. The next day, the membranes were incubated with the corresponding secondary antibodies (Cat. #SA00001-1/SA00001-2; Proteintech; 1:2000) at room temperature for 1 h. Subsequently, the protein bands were visualized using enhanced chemiluminescence (ECL) reagent (share- Biotechnology, Shanghai, China).

Co-IP experiments were conducted following established protocols. U87 cells were promptly eliminated once their occupancy exceeded 90% using a cell scraper and immunoprecipitation lysis buffer containing phenylmethanesulfonyl fluoride (PMSF) and protease inhibitor. The scraped cells were centrifuged, and the supernatant was discarded. Each sample was then supplemented with 1 ml of IP lysate and 10 μl of each of the three protein inhibitors. After the reaction was incubated for 3 hours at 4°C on a rotator, the samples were centrifuged at 12,000 g for 10 minutes at 4°C, and the supernatant, containing the total protein, was collected. From this, 45 μl of the total protein was set aside as the input. The remaining protein was divided into two parts: one treated with S100A8 antibody and the other with IgG as a negative control. Both aliquots were placed on a rotator at 4°C and rotated overnight at 14 rpm. Next, 35 μL of protein A/G beads was added to each immunoprecipitation mixture, which was then gently rocked at 4°C overnight. After being washed five times with cold Co-IP buffer, the mixtures were treated with 2 SDS sample buffers for denaturation the following day. Following the collection of the supernatants, SDS–PAGE was conducted for western blot analysis.

2.8. Cell viability (CCK-8) assay

In 96-well plates, 2000 cells/well from various groups were seeded for the CCK-8 assay. Each day for five days, CCK-8 reagent was added to every well at a consistent time, and the cells were incubated at 37°C for a duration of 2 h. Then, the absorbance was determined using a microplate reader in single-wavelength mode (450 nm). All experiments were repeated three times.

2.9. Wound healing assay

The cells were placed in 6-well plates with 2 mL of culture medium that included 10% FBS. Subsequently, they were cultivated for 24 hours. Once the cells reached 95–100% confluence, a sterile 200 μl pipette tip was used to create vertical scratches across the cell monolayer. After rinsing the detached cells away with PBS, 2 mL of medium without serum was added to the remaining cells for 48 h to allow for cell growth. For each experimental condition, cells in three random fields images were photographed both at the beginning of the experiment and after 48 hours using an Olympus light microscope (magnification, ×40). The experiments were repeated three times.

2.10. Invasion assay

To perform the invasion assay, the filter was precoated with 50 μL of Matrigel, which was diluted using ice-cold serum-free medium at a ratio of 1:8. Subsequently, the Transwell chambers were incubated at 37°C for 1 hour. The upper chamber was then seeded with 4×10^4 cells (U87/U251/HMC3) in 100 μL of McCoy's 5A medium without FBS, while the bottom chamber was filled with 500 μL of medium containing 10% FBS. The cells were cultured at 37°C for 48 hours, and the cells located on the upper surface of the filter were removed with a cotton swab. Moreover, cells that moved to the opposite side of the filter were immobilized using 4% paraformaldehyde at room temperature for 20 min. Subsequently, they were stained with 0.1% crystal violet for 20 minutes. Following the removal of excess crystal violet using PBS, the cells in five randomly selected fields were observed and photographed under a microscope at 200× magnification, and then the results were quantified.

2.11. Co-culture of glioma cells with microglia

For the co-culture system of U87/U251 and HMC3 cells, Transwell chambers from Corning Inc. with a pore size of 0.4 μm were utilized in a 6-well plate. To summarize, HMC3 cells were placed in 6-well dishes at a density of 2×10^5 cells per well. Glioma cells were seeded into the upper chamber of the Transwell at a density of 1×10^5 cells per well. The cells were then incubated overnight to facilitate attachment. Next, HMC3 cells were added to the lower compartments and incubated at 37°C for 48 hours. Subsequently, the HMC3 cells were collected for analysis using RT–qPCR and western blotting techniques.

2.12. Enzyme-linked immunosorbent assay (ELISA)

To evaluate the levels of IL-10 in the cellular supernatant, ELISA was conducted using a commercial kit (Bio-Swamp, China) according to the manufacturer's guidelines. The sample was directly added to each well of the 96-well plate previously coated with the anti-human IL-10 antibody provided in the kit. Finally, the measurements of absorbance at a wavelength of 450 nm were taken using a spectrophotometer designed for reading microplates (Molecular Devices VersaMax, Silicon Valley, USA). The levels of IL-10 were determined using a standard curve.

2.13. Bioinformatics analysis

To assess the clinical value of S100A8, expression level analysis, Kaplan–Meier curve analysis and receiver operating characteristic

(ROC) curve analysis were employed utilizing datasets from The Cancer Genome Atlas (TCGA) and Chinese Glioma Genome Atlas (CGGA). UALCAN software was utilized to examine the protein expression of S100A8 in GBM utilizing data acquired from the Clinical Proteomic Tumor Analysis Consortium (CPTAC). A previously published method was used to assess immune infiltration and molecular interactions.[22]

2.14. In vivo *xenograft assay*

In this study, BALB/C nude mice were purchased from the Animal Experimental Center of Fudan University Shanghai Cancer Center. U87 cells (1×10^5 cells, 0.1 ml PBS) stably transfected with sh-S100A8 were used to establish an orthotopic xenotransplantation model of 6-week-old BALB/c nude mice. To construct a mouse model of microglial clearance, PLX5622 (a colony stimulating factor-1 receptor inhibitor) was added to the diet of mice at 1200 mg/kg from one week before the start of the experiment to the end of the experiment. At the end of the experiment, the growth of intracranial tumors was monitored using *in vivo* bioluminescence imaging.

2.15. *Statistical analysis*

Statistical analysis of the data was conducted using GraphPad Prism 9.0 (GraphPad Software, USA) and SPSS 19.0 software (SPSS, Chicago, IL, USA). The information was recorded as the average standard error of the mean. Independent sample *t*-test or Wilcoxon rank sum test was used for the two groups, and one-way analysis of variance (ANOVA) or Kruskal–Wallis test was used for the comparison of multiple groups. The association between S100A8 expression and clinicopathological traits was analyzed using the chi-squared ($\chi2$) test, and a P value less than 0.05 was considered to indicate statistical significance.

3. Results

3.1. *S100A8 was upregulated in glioma and was associated with poor prognosis*

To identify the role of S100A8 in the progression of glioma, we detected the expression of S100A8 protein in glioma tissue. IHC staining revealed that the expression of S100A8 in glioma tissue was higher than that in normal tissue ($P < 0.05$, Fig. 1A). Subgroup analysis indicated that the expression of S100A8 was associated with glioma grade. S100A8 expression was higher in high-grade glioma (grade III-IV) tissue than in low-grade glioma (grade I-II) ($P < 0.05$, Fig. 1B, Table 1). Additionally, the UALCAN tool was employed to gauge the overall protein expression of S100A8 in GBM tumor and normal tissues. The analysis revealed a substantial increase in S100A8 expression levels within primary tumor samples compared to normal tissues ($P < 0.01$, Fig. 1C).

Subsequently, we evaluated the relationship between S100A8 expression and clinicopathological factors across various carcinoma types in the CGGA and TCGA databases. Specifically, the expression of S100A8 was associated with factors including sex, grade, IDH mutation and 1p19q deletion. S100A8 was more highly expressed in the > 45 years old group than in the <45 years old group. In addition, S100A8 expression was higher in the IDH wild type and 1p19q-non-codel type glioma groups than in the IDH mutant and 1p19q-codel groups, respectively (Supplementary Fig. 1B and C).

Furthermore, with data on S100A8 expression and patient prognosis from the TCGA and CGGA databases, Kaplan–Meier survival analysis was conducted and revealed that glioma patients with high S100A8 expression had a poorer prognosis than those with low expression ($P < 0.05$). This result was confirmed in the GEO database (GSE4271; GSE4412, Supplementary Fig. 2). In addition, receiver operating characteristic (ROC) analysis yielded an area under the curve of 0.761 (95% CI, 0.722–0.800) for S100A8, indicating its potential diagnostic utility. This underscores the plausible predictive significance of S100A8 in glioma diagnosis (Fig. 1F).

3.2. *S100A8 promotes the proliferation, migration and invasion of glioma cells* in vitro

The expression levels of S100A8 in the U87 cell line were higher than those in the U251 cell line ($P < 0.05$, Fig. 2A). Then, cell lines with S100A8 overexpression and knockdown were constructed and verified at the protein and mRNA levels (Fig. 2B and C). Transfection efficiency was verified via fluorescence microscopy (Fig. 2D).

In the CCK-8 assay, overexpression of S100A8 promoted the proliferation of glioma cells, while S100A8 knockdown inhibited the proliferation of glioma cells ($P < 0.01$, Fig. 2E). In addition, the results of wound healing and Transwell experiments suggested that overexpression of S100A8 enhanced the invasion and migration ability of glioma cells, while knockdown of S100A8 had the opposite effect (Fig. 2F and G; $P < 0.05$).

3.3. *S100A8 expression is associated with tumor microenvironment characteristics*

Our exploration commenced with a meticulous examination of differentially expressed genes between samples with high and low S100A8 expression in the TCGA glioma dataset. The volcano plot of the results is depicted in Fig. 3A; it showed 1514 upregulated genes and 508 downregulated genes (Fig. 3B). GO enrichment analysis was performed for these differentially expressed genes. Notably, the S100A8-associated genes in glioma were predominantly enriched in immune-related pathways, mostly notably in the neutrophil activation and immune receptor activation pathways (Fig. 3C). The relationship between S100A8 expression and the abundance of infiltrating immune cells was explored, and a noteworthy association was found between S100A8 expression and the levels of immune cell types such as neutrophils and macrophages (Fig. 3D). In addition, the relationship between S100A8 and microglial infiltration level was explored in the TIMER2.0 database, and the results suggested a robust correlation between S100A8 expression and infiltrating macrophage levels in GBM (Fig. 3E; $r = 0.458$; $P = 1.84E\text{-}08$). Significantly, our analysis revealed that S100A8 expression exhibited a positive correlation with the M2-type macrophage phenotype (ARG1, CD163, CD68, MRC1, MSR1), while conversely, it demonstrated a negative correlation with the M1-type macrophage phenotype (CD80, CD86, IL12B, NOS2) (Fig. 3F). Accordingly, data from the GEPIA2021 database showed marked discrepancies in S100A8 expression levels between M2 and M1 microglia in gliomas (Fig. 3G). These findings collectively suggest that elevated S100A8 expression potentially heralds the transition from M1-type to M2-type macrophage polarization.

To validate this hypothesis, the single-cell level expression of S100A8 in GBM tumors was examined within the microenvironment via the GEO database (GSE84456) (Fig. 3H). Remarkably, our analysis demonstrated heightened S100A8 expression within M2 microglia, with negligible expression observed in M1 microglia (Fig. 3I).

3.4. *S100A8 drives M2 polarization of microglia*

Then, we performed coculture experiments using the HMC3 microglial cell line and U87 glioma cells within a Transwell system (Fig. 4A). By evaluating the migration ability of cocultured microglia through Transwell and wound healing assays, we revealed that S100A8 knockdown in U87 cells substantially decreased the migration capacity of HMC3 microglia ($P < 0.05$, Fig. 4B and C). Our subsequent analyses encompassed the expression of M1/M2 markers. At the gene expression level, the results indicated no notable shifts in the mRNA expression levels of the M1 markers CD68, CD80, and NOS2. However, the mRNA ex-

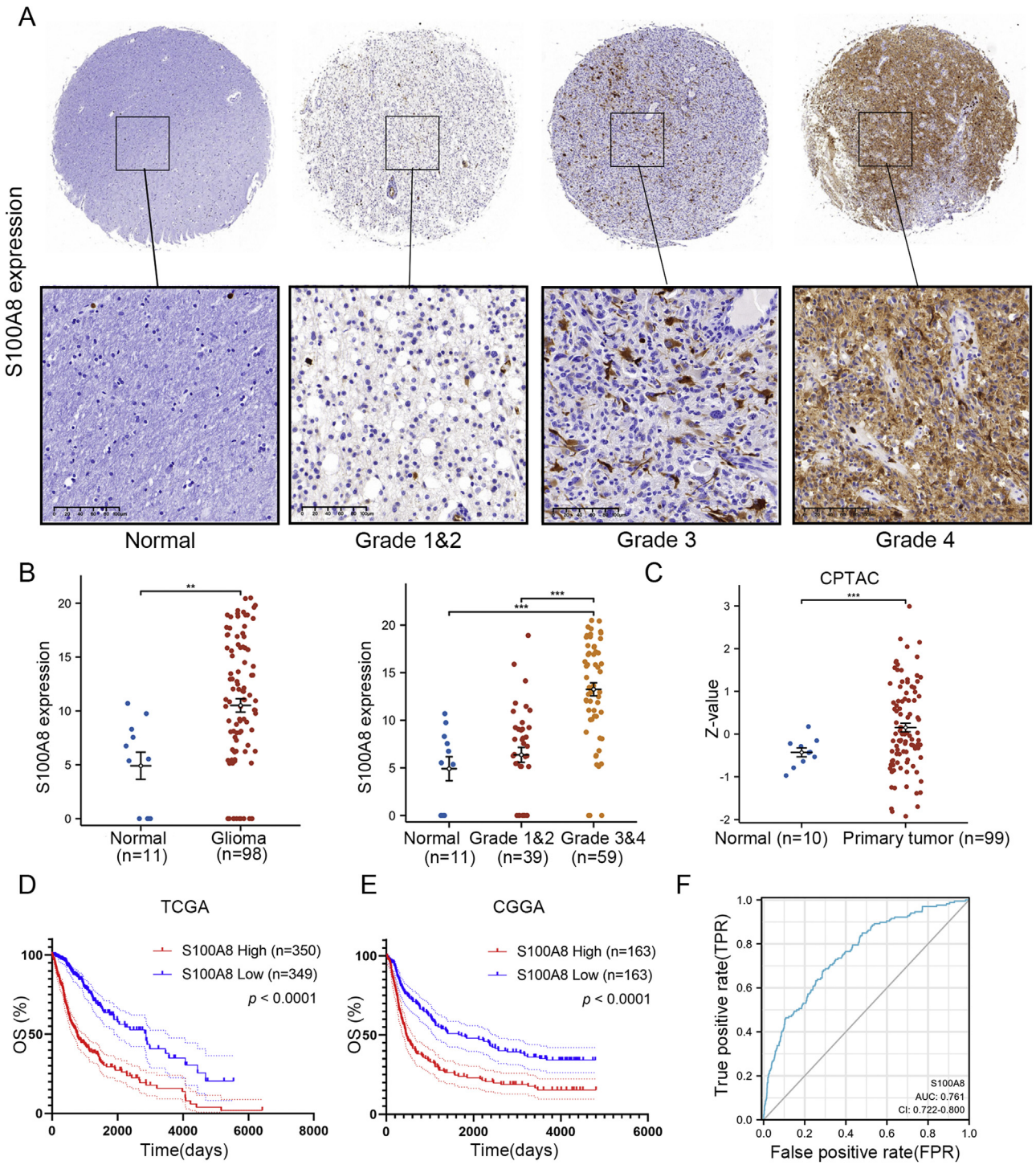

Fig. 1. S100A8 is upregulated in glioma tissue and associated with poor prognosis. (A) Immunohistochemical analysis of S100A8 protein in glioma tissue microarray. Scale bar, 100 μm. (B) immunohistochemistry quantitative analysis. (C) S100A8 expression in CPTAC dataset of 10 normal tissues and 99 glioma tissues. (D) Association of S100A8 with prognosis in the TCGA cohort. (E) Association of S100A8 with prognosis in the CGGA cohort. (F) ROC curve analysis of S100A8 in glioma using TCGA datasets. OS, overall survival. *, $P < 0.05$; **, $P < 0.01$; ***, $P < 0.001$.

pression levels of the M2 markers CD163, ARG1, and MRC1 decreased in the siS100A8 group and increased in the S100A8 overexpression group compared to the negative control (NC) group (Fig. 4D). Similarly, western blot analysis revealed decreased CD163 and ARG1 protein expression in the siS100A8 group, while the S100A8 overexpression group demonstrated elevated levels of CD163 and ARG1 protein compared to the NC group (Fig. 4E).

3.5. S100A8 promoted the secretion of IL-10 by interacting with TLR4

The analysis of genes related to S100A8 and microglial polarization using the STRING and GeneCards databases suggested that TLR4 and IL-10 may be important molecules involved in microglial polarization (Fig. 5A and B). Knockdown of S100A8 led to a decrease in the expression level of IL-10, and overexpression of S100A8 increased the expres-

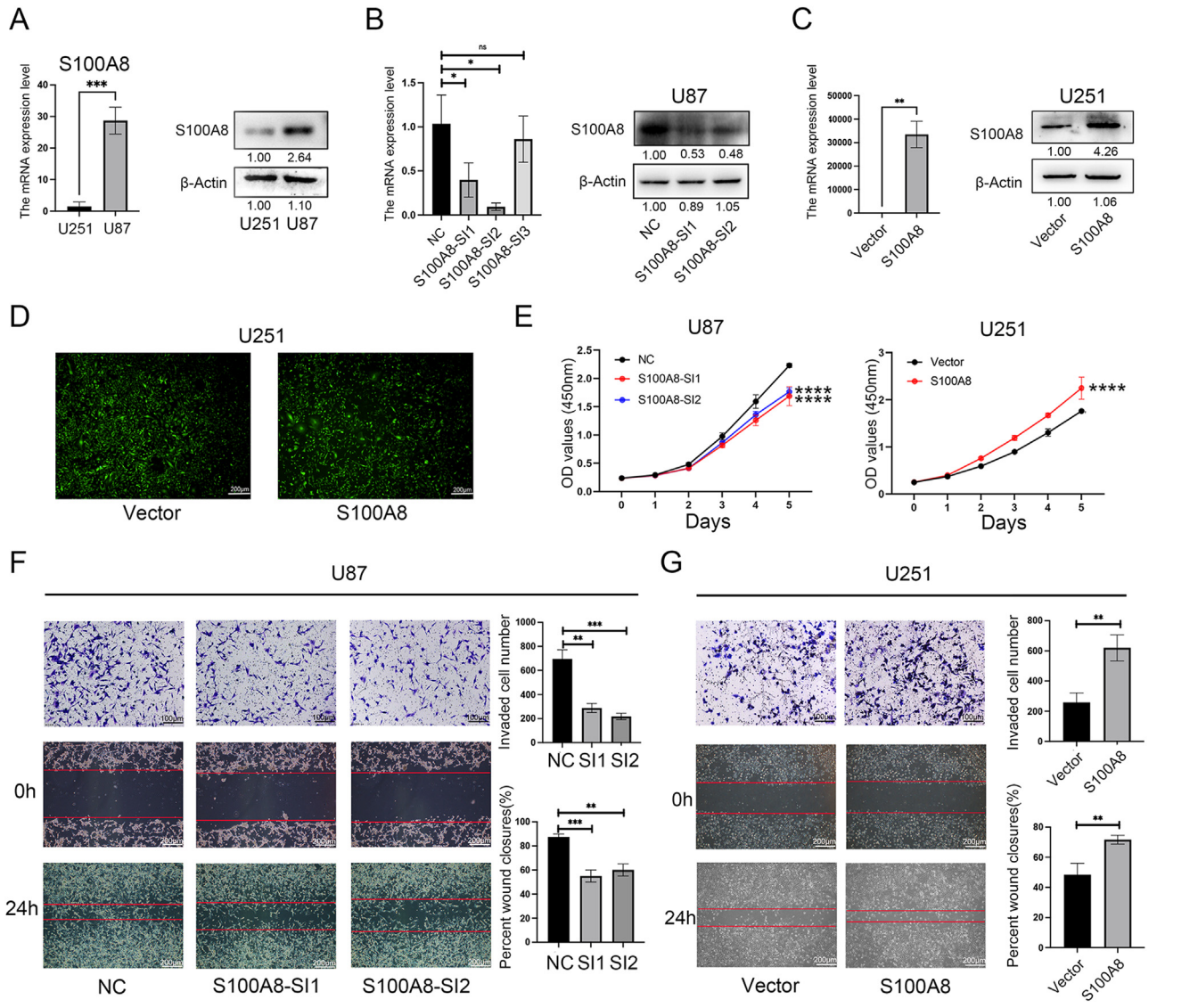

Fig. 2. Effect of S100A8 knockdown and overexpression on glioma cell function. (A) S100A8 protein and mRNA expression levels in two glioma cell lines U87 and U251. (B, C) U87 and U251 cells transfected with siS100A8 or plasmids carrying S100A8 cDNA and then subjected to Western blot analysis and qPCR of S100A8 expression. (D) Fluorescence microscopy verified the transfection efficiency of U251 into S100A8 plasmid. Scale bar, 200 μm. (E) The effect of knockdown or overexpression of S100A8 on cell proliferation was investigated using CCK-8 assay. (F, G) The migration and invasion function of glioma cells were evaluated by wound-healing assay (scale bar, 200 μm) and Transwell assay (scale bar, 100 μm). OD, optical density. *, $P < 0.05$; **, $P < 0.01$; ***, $P < 0.001$.

sion level of IL-10, but S100A8 expression did not affect the expression level of TLR4 (Fig. 5C). At the same time, IL-10 in glioma supernatants was examined using ELISA. The results indicated that S100A8 downregulation reduced the expression of IL-10 in the supernatant of U87 cells, and the overexpression of S100A8 had the opposite effect (Fig. 5D).

Based on our bioinformatics analysis and previous research conclusions, Co-IP experiments confirmed that S100A8 could interact with TLR4 (Fig. 5E). Immunofluorescence confocal microscopy of U87 cell lines also confirmed the colocalization of S100A8 and TLR4 (Fig. 5F). Moreover, we treated U87 and U251 cells with TLR4-IN-C34, a specific inhibitor of TLR4. In addition, western blotting and ELISA were used to detect the expression levels of IL-10 in and out of cells. The results indicated that the expression levels of IL-10 decreased after inhibition of TLR4 by C34 (Fig. 5G and H). At the same time, glioma cells treated with inhibitors were cocultured with microglia to detect mRNA expression levels of M1 and M2 markers. C34 reversed microglial polarization caused by S100A8 overexpression (Fig. 5I).

3.6. S100A8 activates the TLR4/NF-kB and JAK1/STAT3 signaling pathways in the glioma microenvironment

The KEGG pathway enrichment analysis revealed that S100A8 potentially influences the NF-κB and JAK/STAT signaling pathways (Fig. 6A). Utilizing lentiviral transfection technology, we successfully established a cell line with stable S100A8 silencing. Upon verification of the knockdown efficiency at the protein level, we proceeded to coculture the altered cell line with microglia. Western blot analysis was employed to assess the effects on the JAK1/STAT3 and NF-κB pathways. Our findings indicated that the silencing of S100A8 can suppress NF-κB pathways in glioma and inhibit the JAK1/STAT3 pathway in microglia (Fig. 6B). In addition, under the stimulation of TLR4 inhibitors, the NF-κB pathway in glioma cells was significantly inhibited, and TLR4 could inhibit the activation of NF-κB pathway by S100A8 overexpression (Fig. 6C). We implanted Luciferase-labeled sh-S100A8 glioma cells into nude mice to establish an intracranial mouse model. Tumor growth was monitored using an *in vivo* imaging system. The results showed

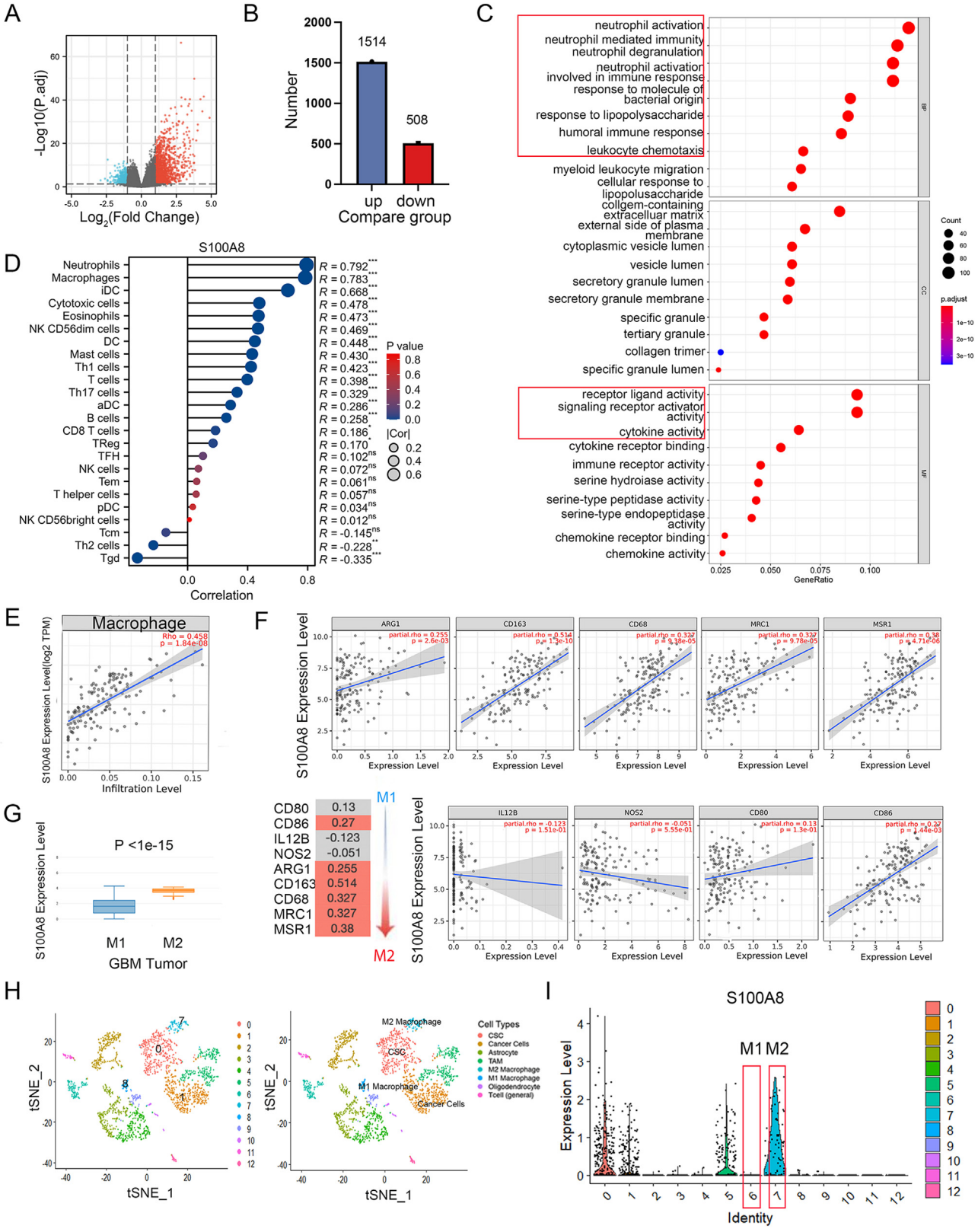

Fig. 3. S100A8 was associated with an immune response. (A and B) The volcano plot showed differential expressed gene of S100A8 in TCGA. (C) Go enrichment analysis. (D) Relationship between S100A8 expression and immune cell infiltration. (E) Relationship between S100A8 expression and macrophage in glioma. (F) S100A8 was correlated with the expression of macrophage M1 and M2 markers in the TIMER2.0 database. (G) The expression of S100A8 in different polarized macrophages was included in the GEPIA2021 database. (H, I) The expression of S100A8 in various cells is distributed at the single-cell level.

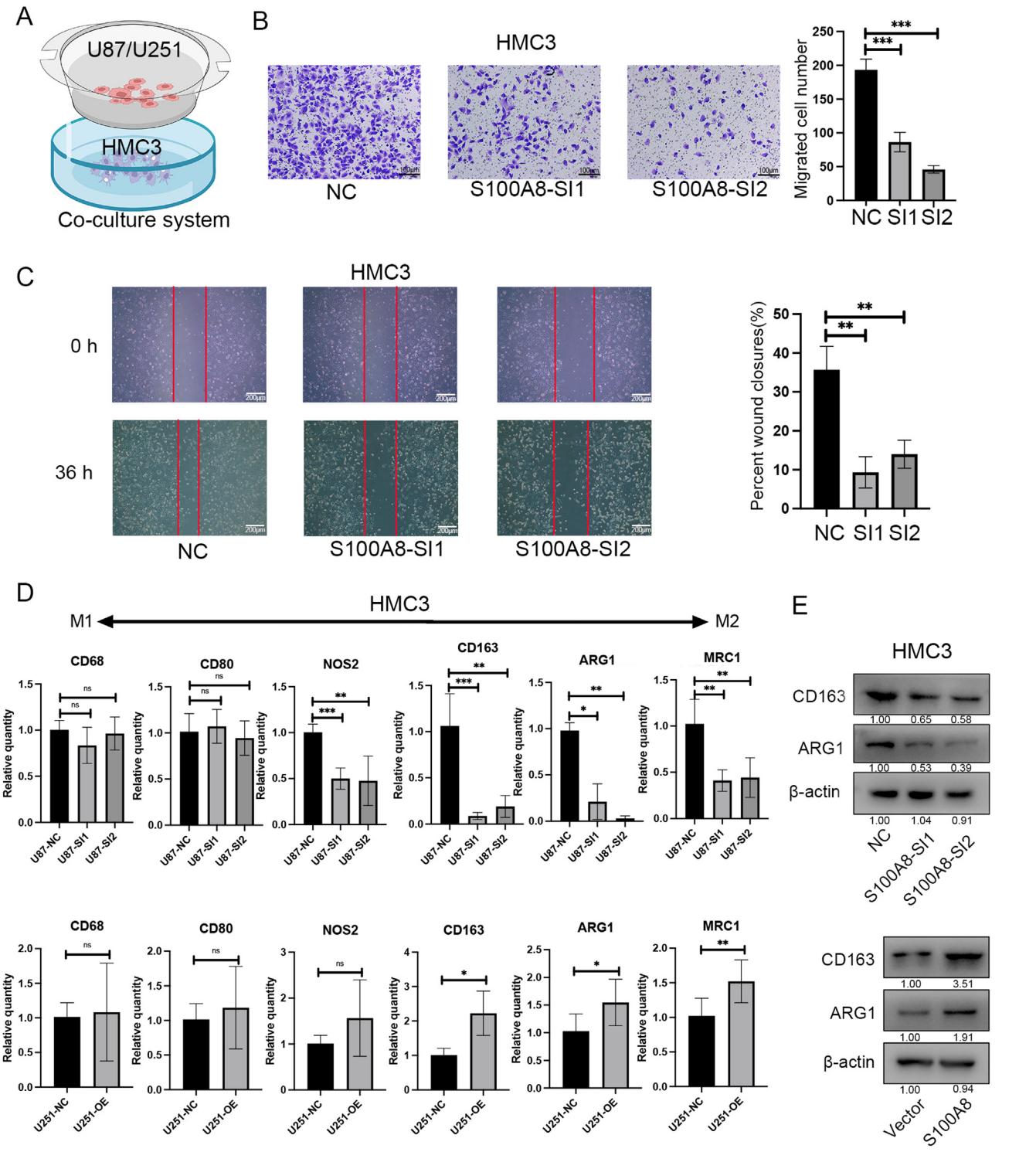

Fig. 4. S100A8 promotes microglial infiltration and polarization. (A) Model diagram of co-culture system. (B) Transwell assay. U87 cells were grown and transiently transfected with siS100A8 or control siRNA, and co-culture with microglia HMC3, then subjected to the Transwell assay. Scale bar, 100 μm. (C) Wound-healing assay. U87 was co-cultured with microglia HMC3 after S100A8 knocked down. Then subjected to the assay. Scale bar, 200 μm. (D) The mRNA expression level of the M1 and M2 markers of HMC3 co-cultured with U87 or U251 cells were detected by qPCR. (E) The protein expression level of M2 markers of HMC3 were detected by Western blot. *, $P < 0.05$; **, $P < 0.01$; ***, $P < 0.001$.

that the knockdown of S100A8 could significantly suppress the *in vivo* growth of glioma, suggesting the important role of S100A8 in glioma development (Fig. 6D). In order to verify that S100A8 affects glioma cell progression through microglia, we used colony stimulating faction-1 receptor inhibitor PLX5622 in mouse to eliminate microglia. The shS100A8–1 and shS100A8-NC cells were respectively injected into the mice treated with PLX5622. The results indicated that the tumor burden of PLX5622+shS100A8-NC group and PLX5622+shS100A8–1 group was lower than that of the control group, and no significant difference between the two treatment groups (Fig. 6E). In addition, immunofluores-

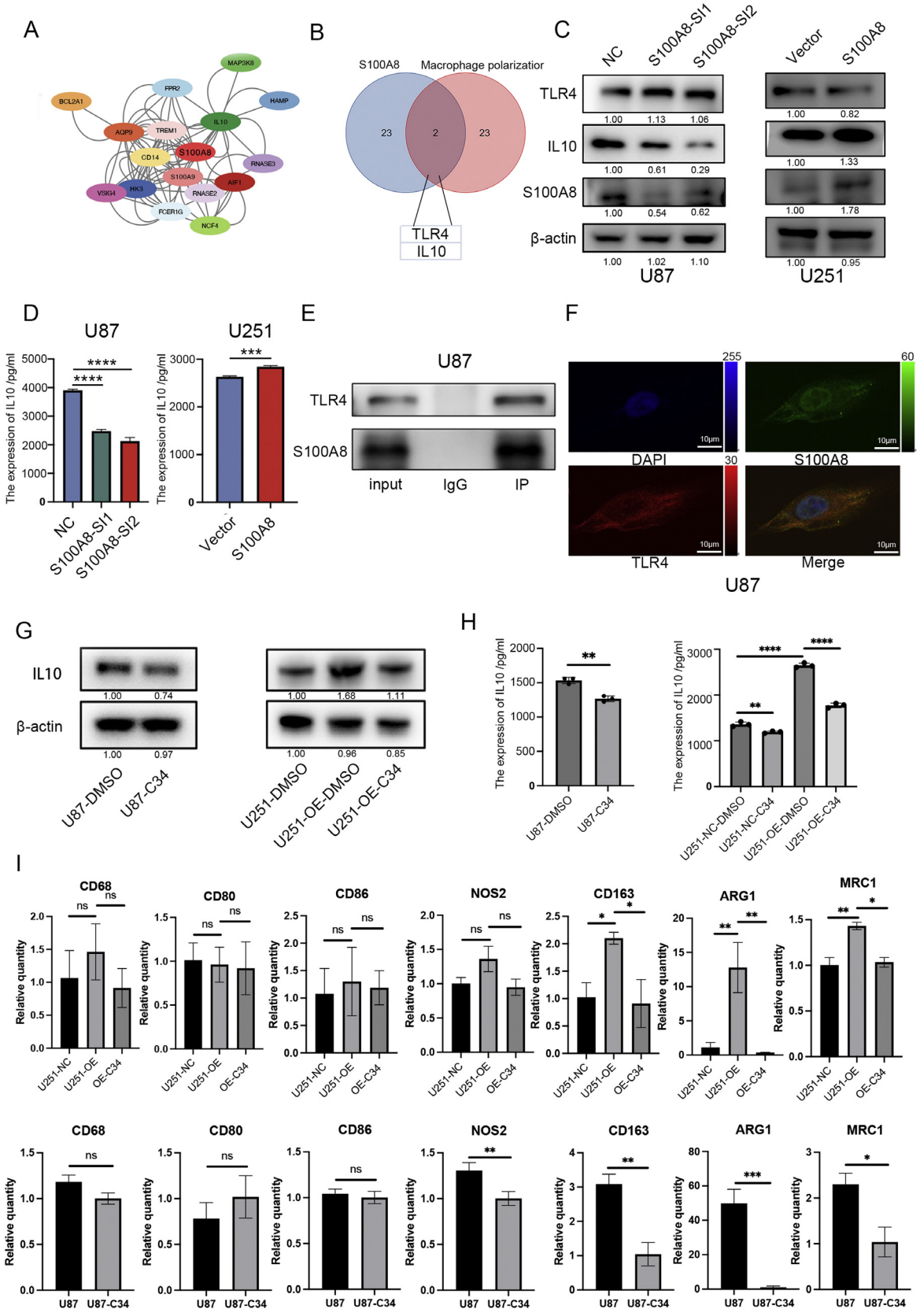

Fig. 5. S100A8 binds TLR4 to promote IL-10 secretion. (A) Cytoscape was used to build the protein-protein interaction network of co-expressed genes. (B) Genecards was used to explore genes related to S100A8 and macrophage polarization. (C) Western blot was used to detect the expression levels of TLR4 and IL-10 after S100A8 knockdown and overexpression. (D) The content of IL-10 in cell supernatant was detected by ELISA. (E, F) Verify the combined ability of the S100A8 and TLR4 using coimmunoprecipitation and immunocytochemistry. Scale bar, 10 μm. (G, H) After adding TLR4 inhibitor TLR-IN–C34, the content of IL-10 in and out of cells was detected by Western blot and ELISA. (I) After treatment with TLR4 inhibitors, glioma cells were co-cultured with microglia, and the mRNA expression levels of M1 and M2 markers were detected by qPCR. *, $P < 0.05$; **, $P < 0.01$; ***, $P < 0.001$.

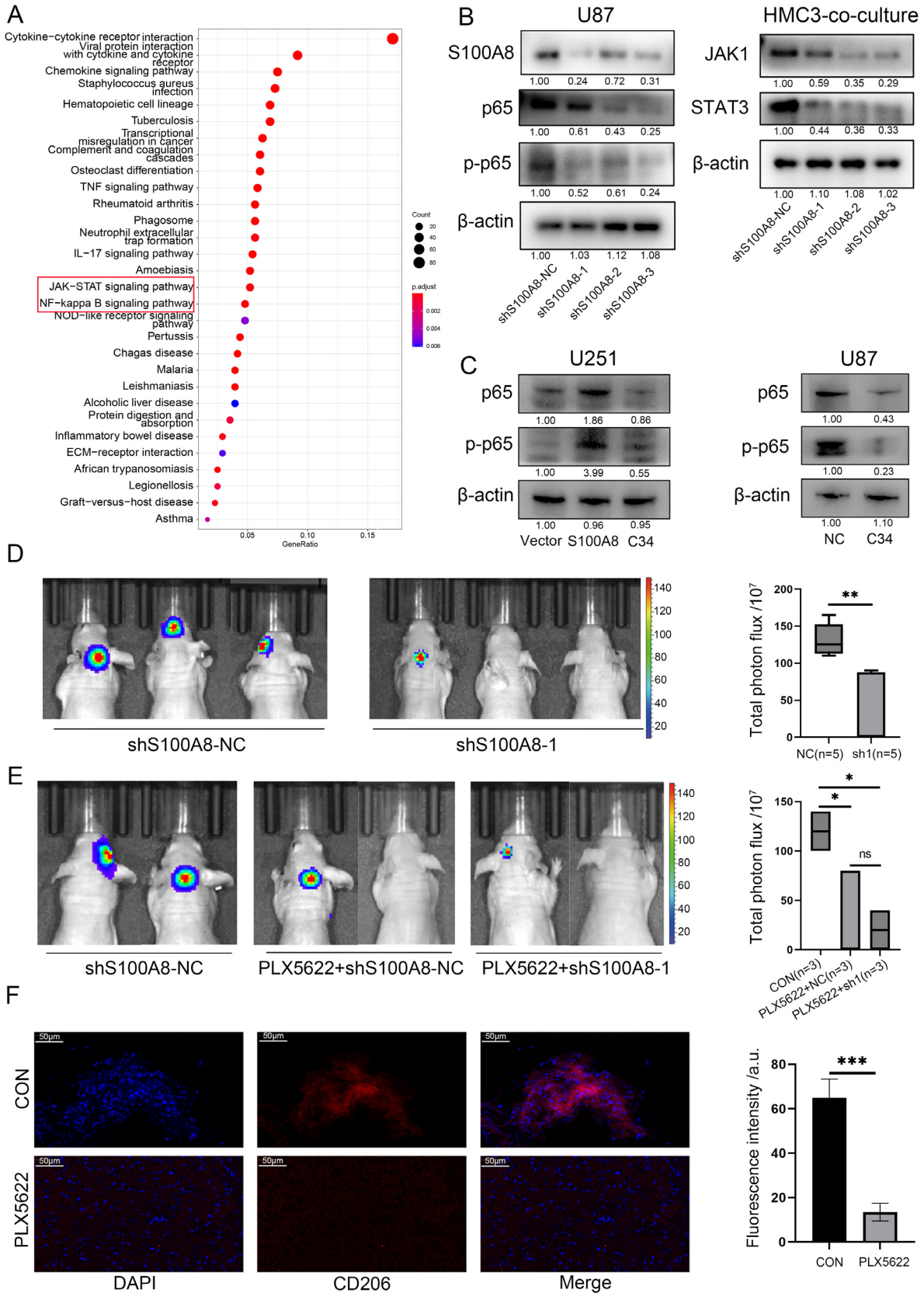

Fig. 6. S100A8 can activate the NF-kB and JAK-STAT signaling pathways. (A) KEGG enrichment analysis of differential genes related to S100A8 in glioma. (B) Western blot was used to detect the target proteins of NF-κB and JAK-STAT in glioma and microglia cell lines. (C) Western blot was used to detect the target proteins of NF-kB in glioma. (D and E) Intracranial xenograft tumor growths with different treatment as indicated respectively were examined by bioluminescent images (left panels) and quantified by the fluorescence intensity (right panels). (F) Immunofluorescence staining verified the difference of CD206 expression. Scale bar, 50 μm. *, $P < 0.05$; **, $P < 0.01$; ***, $P < 0.001$. Con, control; NC, negative control; sh1, shS100A8-1.

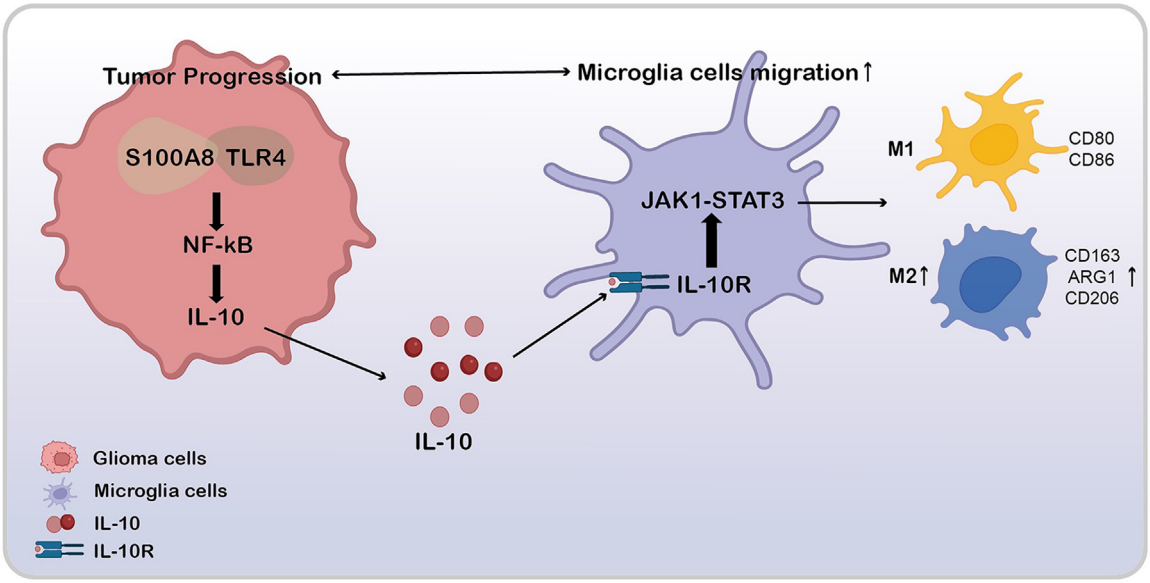

Fig. 7. Schematic of function and regulatory mechanism of S100A8 in glioma immune microenvironment.

cence staining was performed on the brain tissue sections of the control group and the PLX5622 group. The result showed that the expression of CD206 in microgila, a marker of M2 polarization, was higher in the control group than that in the PLX5622 group (Fig. 6F). These results suggest that S100A8 affect the development of glioma by influencing microglial polarization. To graphically summarize these observations, we provide a diagram that illustrates the functional impact and regulatory mechanisms exerted by S100A8 within the glioma immune microenvironment (Fig. 7).

4. Discussion

The intracranial tumor microenvironment (TME) is devoid of immune cells such as T and B lymphocytes but is rich in TAMs, primarily brain microglia.[13,14] Tumor cells are capable of interacting with microglia, a process that contributes to the growth of these tumors.[23] Recent research has highlighted that TAMs play a pivotal role in glioma growth and progression. The unique metabolic characteristics of glioma serve as an important means for communication with the surrounding TME, promoting the secretion of related chemokines and cytokines to regulate immune cell function and chemotaxis, ultimately leading to tumorigenesis, development, migration, invasion, recurrence and drug resistance.[15,16] Previous studies have suggested that microglial polarization in the glioma microenvironment can promote the progression of glioma, and inhibiting or reversing this polarization can block the progression of glioma by blocking the Gal-9/Tim-3 signal or inhibiting the CSF-1R signaling pathway.[24–26] Hence, it is of paramount importance to investigate the intricate interactions between glioma cells and microglia in the context of tumor research.

S100A8 is considered an important oncogene in a variety of cancers, such as breast cancer and ovarian cancer, and is significantly associated with a poor prognosis.[10,27–29] However, there is a lack of comprehensive research investigating the function and mechanism of S100A8 in the occurrence and progression of glioma. Therefore, we evaluated the expression of S100A8 in 98 distinct glioma samples. In addition, the expression of S100A8 and its association with pathological factors were also investigated. Our study revealed that S100A8 expression was elevated in glioma tissues and correlated with higher pathological grades. Furthermore, higher S100A8 expression was associated with poor prognosis, suggesting that S100A8 might be a prognostic indicator. Through a combination of bioinformatic analysis and experimental methods, we explored the potential mechanism by which S100A8 promotes glioma development, with a focus on its involvement in microglial cell polarization.

A previous study reported the broad biological functions of S100A8 in inflammatory processes and immune responses. Recently, researchers have found a potential role of S100A8 in regulating cancer progression. In this study, a series of bioinformatics analyses and experimental results suggested that S100A8 could promote microglial M2 polarization. S100A8 was not only highly expressed in glioma but also promoted tumor progression by regulating microglial M2 polarization. Moreover, we identified IL-10 as the key molecule by which S100A8 promotes microglial polarization. IL-10 is a crucial cytokine for immune regulation and exerts significant anti-inflammatory effects on various immune cells, thereby mitigating excessive tissue damage caused by inflammation. Previous research has demonstrated that IL-10 could induce the transformation of macrophages into the M2 phenotype in tumors and in response to different stimuli such as injury and inflammation, consequently establishing an immunosuppressive microenvironment.[30] We evaluated both intracellular and extracellular IL-10 levels in U251 and U87 glioma cell lines with either overexpression or knockdown of S100A8. The data revealed that S100A8 overexpression upregulated IL-10 expression intracellularly and extracellularly, whereas S100A8 knockdown decreased IL-10 levels. These findings imply that S100A8 facilitates M2 microglial polarization by augmenting IL-10 expression and secretion.

Previous studies have revealed that TLR4 is closely related to macrophage polarization.[31,32] TLR4 could promote macrophage polarization and be a target for blocking these processes.[33] TLR4 encodes a protein that belongs to the TLR family, which is essential for recognizing pathogens and initiating innate immune responses. TLR4 plays a significant role in tumorigenesis and chronic inflammation. Its involvement in glioma has also been extensively reported. Upon binding to its ligand in tumor cells, TLR4 could activate intracellular cascades, thereby promoting cytoplasmic signaling.[34–36] In addition, previous studies have shown that targeted inhibition of S100A8 or inhibition of upstream molecules of S100A8 can inhibit TLR4 signaling pathway and then regulate macrophage phenotype and control disease progression in a variety of diseases, including cirrhosis, diabetic nephropathy, and tumors.[37–39] In our study, we demonstrated for the first time that S100A8 specifically interacts with TLR4 in gliomas. When we treated glioma S100A8-overexpressing cells with TLR4-IN–C34, a specific inhibitor of TLR4,

we observed a reduction in IL-10. Furthermore, following coculture of glioma cells treated with TLR4-IN–C34 with microglia, we observed a suppression of the microglial M2 polarization phenotype. This suggests that S100A8 promotes IL-10 secretion through specific binding to TLR4 and that this process can be inhibited by TLR4 inhibitors.

To determine which pathway is activated upon S100A8 binding with TLR4 to promote IL-10 secretion, we performed KEGG enrichment analysis. The results suggest that S100A8 is involved in the NF-κB and JAK/STAT pathways, two classical immune-related pathways. NF-κB is a critical transcription factor in multiple immune response pathways and can stimulate the production of various inflammatory mediators.[40] Then, we experimentally verified that the activation of NF-κB was significantly correlated with the expression of S100A8 in glioma. This suggests that S100A8 combined with TLR4 could activate the NF-κB pathway. In addition, previous studies have shown that IL-10 can bind to IL-10R on the cell surface to activate STAT3.[41,42] Consequently, we posited that elevated IL-10 secretion, spurred by the increased expression of S100A8 within the glioma tumor microenvironment, induces the JAK1/STAT3 pathway in microglia. This process results in the release of immunosuppressive cytokines, thereby remodelling the immune landscape of the tumor. To corroborate this hypothesis, we employed a Transwell system for the coculture of glioma cells and microglia and then assessed the expression profiles of JAK1/STAT3 pathway components in microglia. The data from our inquiry indicated that, within the coculture framework using S100A8-deficient cell lines, there was a noticeable inhibition of the JAK1/STAT3 pathway in microglia.[43]

Drawing on robust evidence, our research highlights the critical role of S100A8 in glioma progression. Specifically, our findings indicate that S100A8 stimulates NF-κB pathway activation through interaction with TLR4, culminating in elevated IL-10 production. This increase in IL-10 activates the JAK1/STAT3 signaling pathway in microglia, fostering their transition to an M2 phenotype. Notably, these findings highlight the potential of S100A8 as a novel target of microglial polarization therapies for glioma.

Declaration of competing interest

The authors declare that they have no known competing financial interests or personal relationships that could have appeared to influence the work reported in this paper.

Ethics statement

It was conducted in compliance with the principles of the Declaration of Helsinki and approved by ethics committee of the Fudan University Shanghai Cancer Center (approval number: 050432-4-1911D). Written informed consent was obtained from all the participants. Mouse-related studies were approved by the Institutional Animal Care and Use Committee of Fudan University Shanghai Cance Center (approval number: FUSCC-IACUC-2023469).

Acknowledgments

This work was supported by the National Natural Science Foundation of China (grant numbers: 82103429 and 82173177).

Author contributions

Y.Y., C.H., C.Y. and G.Y. conducted the conception and design and administrated the support. Y.Y., L.L., F.M., Z.C., C.L. and L.D. performed provision of study materials or patients, collection and assembly of data, data analysis and interpretation. Y.Y., L.Y. and C.X. conducted graphs plotting. Y.Y., C.Y. and G.Y. drafted and revised this manuscript.

Supplementary materials

Supplementary material associated with this article can be found, in the online version, at doi:10.1016/j.jncc.2024.07.001.

References

1. Alexander BM, Cloughesy TF. Adult glioblastoma. *J Clin Oncol*. 2017;35(21):2402–2409. doi:10.1200/JCO.2017.73.0119.
2. Shergalis A, Bankhead A, Luesakul U, Muangsin N, Neamati N. Current challenges and opportunities in treating glioblastoma. *Pharmacol Rev*. 2018;70(3):412–445. doi:10.1124/pr.117.014944.
3. Jackson CM, Choi J, Lim M. Mechanisms of immunotherapy resistance: lessons from glioblastoma. *Nat Immunol*. 2019;20(9):1100–1109. doi:10.1038/s41590-019-0433-y.
4. Karachi A, Dastmalchi F, Mitchell DA, Rahman M. Temozolomide for immunomodulation in the treatment of glioblastoma. *Neuro Oncol*. 2018;20(12):1566–1572. doi:10.1093/neuonc/noy072.
5. Uddin MS, Mamun AA, Alghamdi BS, et al. Epigenetics of glioblastoma multiforme: from molecular mechanisms to therapeutic approaches. *Semin Cancer Biol*. 2022;83:100–120. doi:10.1016/j.semcancer.2020.12.015.
6. Agnihotri TG, Salave S, Shinde T, et al. Understanding the role of endothelial cells in brain tumor formation and metastasis: a proposition to be explored for better therapy. *J Natl Cancer Cent*. 2023;;3(3):222–235. doi:10.1016/j.jncc.2023.08.001.
7. Wang S, Song R, Wang Z, Jing Z, Wang S, Ma J. S100A8/A9 in inflammation. *Front Immunol*. 2018;9:1298. doi:10.3389/fimmu.2018.01298.
8. Scott NR, Swanson RV, Al-Hammadi N, et al. S100A8/A9 regulates CD11b expression and neutrophil recruitment during chronic tuberculosis. *J Clin Investig*. 2020;130(6):3098–3112. doi:10.1172/JCI130546.
9. Li S, Zhang J, Qian S, et al. S100A8 promotes epithelial-mesenchymal transition and metastasis under TGF-β/USF2 axis in colorectal cancer. *Cancer Commun (Lond)*. 2021;41(2):154–170. doi:10.1002/cac2.12130.
10. Wang D, Liu G, Wu B, Chen L, Zeng L, Pan Y. Clinical significance of elevated S100A8 expression in breast cancer patients. *Front Oncol*. 2018;8:496. doi:10.3389/fonc.2018.00496.
11. Liao WC, Chen CT, Tsai YS, et al. S100A8, S100A9 and S100A8/A9 heterodimer as novel cachexigenic factors for pancreatic cancer-induced cachexia. *BMC Cancer*. 2023;23(1):513. doi:10.1186/s12885-023-11009-8.
12. Zhang Y, Yang X, Zhu XL, et al. S100A gene family: immune-related prognostic biomarkers and therapeutic targets for low-grade glioma. *Aging (Albany NY)*. 2021;13(11):15459–15478. doi:10.18632/aging.203103.
13. Martins TA, Schmassmann P, Shekarian T, et al. Microglia-centered combinatorial strategies against glioblastoma. *Front Immunol*. 2020;11:571951. doi:10.3389/fimmu.2020.571951.
14. Prinz M, Jung S, Priller J. Microglia biology: one century of evolving concepts. *Cell*. 2019;179(2):292–311. doi:10.1016/j.cell.2019.08.053.
15. Xuan W, Lesniak MS, James CD, Heimberger AB, Chen P. Context-dependent glioblastoma-macrophage/microglia symbiosis and associated mechanisms. *Trends Immunol*. 2021;42(4):280–292. doi:10.1016/j.it.2021.02.004.
16. Dumas AA, Pomella N, Rosser G, et al. Microglia promote glioblastoma via mTOR-mediated immunosuppression of the tumour microenvironment. *EMBO J*. 2020;39(15):e103790. doi:10.15252/embj.2019103790.
17. Dong Z, Cui H. Epigenetic modulation of metabolism in glioblastoma. *Semin Cancer Biol*. 2019;57:45–51. doi:10.1016/j.semcancer.2018.09.002.
18. Sauter G, Simon R, Hillan K. Tissue microarrays in drug discovery. *Nat Rev Drug Discov*. 2003;2(12):962–972.
19. Gao Y, Zheng H, Li L, et al. Prostate-specific membrane antigen (PSMA) promotes angiogenesis of glioblastoma through interacting with ITGB4 and regulating NF-κB signaling pathway. *Front Cell Dev Biol*. 2021;9:598377. doi:10.3389/fcell.2021.598377.
20. Yin M, Xiong Y, Huang L, et al. Circulating follicular helper T cells and subsets are associated with immune response to hepatitis B vaccination. *Hum Vaccin Immunother*. 2021;17(2):566–574. doi:10.1080/21645515.2020.1775457.
21. Tu W, Zheng H, Li L, et al. Secreted phosphoprotein 1 promotes angiogenesis of glioblastoma through upregulating PSMA expression via transcription factor HIF1alpha. *Acta Biochim Biophys Sin (Shanghai)*. 2022;55(3):417–425. doi:10.3724/abbs.2022157.
22. Yang Y, Cui H, Li D, et al. Prognosis and immunological characteristics of PGK1 in lung adenocarcinoma: a systematic analysis. *Cancers (Basel)*. 2022;14(21):5288. doi:10.3390/cancers14215228.
23. Matias D, Predes D, Niemeyer Filho P, et al. Microglia-glioblastoma interactions: new role for Wnt signaling. *Biochim Biophys Acta Rev Cancer*. 2017;1868(1):333–340. doi:10.1016/j.bbcan.2017.05.007.
24. Yu-Ju Wu C, Chen CH, Lin CY, et al. CCL5 of glioma-associated microglia/macrophages regulates glioma migration and invasion via calcium-dependent matrix metalloproteinase 2. *Neuro Oncol*. 2020;22(2):253–266. doi:10.1093/neuonc/noz189.
25. Pyonteck SM, Akkari L, Schuhmacher AJ, et al. CSF-1R inhibition alters macrophage polarization and blocks glioma progression. *Nat Med*. 2013;19(10):1264–1272. doi:10.1038/nm.3337.
26. Ni X, Wu W, Sun X, et al. Interrogating glioma-M2 macrophage interactions identifies Gal-9/Tim-3 as a viable target against PTEN-null glioblastoma. *Sci Adv*. 2022;8(27):eabl5165. doi:10.1126/sciadv.abl5165.
27. Zhang X, Niu M, Li T, et al. S100A8/A9 as a risk factor for breast cancer negatively regulated by DACH1. *Biomark Res*. 2023;11(1):106. doi:10.1186/s40364-023-00548-8.

28. Li Z, McGinn O, Wu Y, et al. ESR1 mutant breast cancers show elevated basal cytokeratins and immune activation. *Nat Commun*. 2022;13(1):2011. doi:10.1038/s41467-022-29498-9.
29. Perego M, Tyurin VA, Tyurina YY, et al. Reactivation of dormant tumor cells by modified lipids derived from stress-activated neutrophils. *Sci Transl Med*. 2020;12(572):eabb5817. doi:10.1126/scitranslmed.abb5817.
30. Mahon OR, Browe DC, Gonzalez-Fernandez T, et al. Nano-particle mediated M2 macrophage polarization enhances bone formation and MSC osteogenesis in an IL-10 dependent manner. *Biomaterials*. 2020;239:119833. doi:10.1016/j.biomaterials.2020.119833.
31. Capitani M, Al-Shaibi AA, Pandey S, et al. Biallelic TLR4 deficiency in humans. *J Allergy Clin Immunol*. 2023;151(3):783–790 e5. doi:10.1016/j.jaci.2022.08.030.
32. Malengier-Devlies B, Metzemaekers M, Gouwy M, et al. Phenotypical and functional characterization of neutrophils in two pyrin-associated auto-inflammatory diseases. *J Clin Immunol*. 2021;41(5):1072–1084. doi:10.1007/s10875-021-01008-4.
33. Li R, Zhou R, Wang H, et al. Gut microbiota-stimulated cathepsin K secretion mediates TLR4-dependent M2 macrophage polarization and promotes tumor metastasis in colorectal cancer. *Cell Death Differ*. 2019;26(11):2447–2463. doi:10.1038/s41418-019-0312-y.
34. Litak J, Grochowski C, Litak J, et al. TLR-4 signaling *vs*. immune checkpoints, miRNAs molecules, cancer stem cells, and wingless-signaling interplay in glioblastoma multiforme-future perspectives. *Int J Mol Sci*. 2020;21(9):3114. doi:10.3390/ijms21093114.
35. Kına I, Sultuybek GK, Soydas T, et al. Variations in Toll-like receptor and nuclear factor-kappa B genes and the risk of glioma. *Br J Neurosurg*. 2019;33(2):165–170. doi:10.1080/02688697.2018.1540764.
36. Hanahan D, Weinberg RA. Hallmarks of cancer: the next generation. *Cell*. 2011;144(5):646–674. doi:10.1016/j.cell.2011.02.013.
37. Hou C, Wang D, Zhao M, et al. MANF brakes TLR4 signaling by competitively binding S100A8 with S100A9 to regulate macrophage phenotypes in hepatic fibrosis. *Acta Pharm Sin B*. 2023;13(10):4234–4252. doi:10.1016/j.apsb.2023.07.027.
38. Du L, Chen Y, Shi J, et al. Inhibition of S100A8/A9 ameliorates renal interstitial fibrosis in diabetic nephropathy. *Metabolism*. 2023;144:155376. doi:10.1016/j.metabol.2022.155376.
39. Deguchi A, Tomita T, Ohto U, et al. Eritoran inhibits S100A8-mediated TLR4/MD-2 activation and tumor growth by changing the immune microenvironment. *Oncogene*. 2016;35(11):1445–1456. doi:10.1038/onc.2015.211.
40. Hu X, Li J, Fu M, Zhao X, Wang W. The JAK/STAT signaling pathway: from bench to clinic. *Signal Transduct Target Ther*. 2021;6(1):402. doi:10.1038/s41392-021-00791-1.
41. Zhang X, Hu B, Sun YF, et al. Arsenic trioxide induces differentiation of cancer stem cells in hepatocellular carcinoma through inhibition of LIF/JAK1/STAT3 and NF-kB signaling pathways synergistically. *Clin Transl Med*. 2021;11(2):e335. doi:10.1002/ctm2.335.
42. Lee H, Herrmann A, Deng JH, et al. Persistently activated Stat3 maintains constitutive NF-kappaB activity in tumors. *Cancer Cell*. 2009;15(4):283–293. doi:10.1016/j.ccr.2009.02.015.
43. Stine RR, Matunis EL. JAK-STAT signaling in stem cells. *Adv Exp Med Biol*. 2013;786:247–267. doi:10.1007/978-94-007-6621-1_14.